

Artificial Intelligence (AI)-Powered Robot for Optical Network Operation Automation

Xiaonan Xu^(1*), Haoshuo Chen⁽²⁾, Michael Scheutzw⁽²⁾, Jesse E. Simsarian⁽²⁾, Roland Ryf⁽²⁾,
Gin Qua⁽²⁾, Amey Hande⁽²⁾, Rob Dinoff⁽²⁾, Mijail Szczerban⁽²⁾, Mikael Mazur⁽²⁾,
Lauren Dallachiesa⁽²⁾, Nicolas K. Fontaine⁽²⁾, Jim Sandoz⁽³⁾, Mike Coss⁽²⁾, and David T. Neilson⁽²⁾

¹ Aberdeen, NJ 07747, USA

² Nokia Bell Labs, 600 Mountain Ave., Murray Hill, NJ 07974, USA

³ Nokia, 600 Mountain Ave., Murray Hill, NJ 07974, USA

*xuxiaonan2008@gmail.com

Abstract: We demonstrate an artificial intelligence (AI)-powered robot for optical network operation automation and showcase three demos: 1) robot-driven event classification, 2) modified LC duplex connector for robotic operation, and 3) AI inference acceleration using an FPGA. © 2024 The Author(s)

1. Overview

Driven by advancements in computer vision and artificial intelligence, robots have made significant progress in handling complex tasks. For example, the automotive industry employs robots for assembly, and warehouses use them for activities like picking and placing items. Recently, we demonstrated an Artificial Intelligence (AI)-powered robot capable of navigating between different network rooms and performing various optical network operations, including fiber switching [1]. In this automated system, the robot first detects a single fiber manipulation event for basic path verification and then physically disconnects fibers by unplugging Lucent Connector (LC) duplex connectors from adapters; Fiber insertion is enabled by a Convolutional Neural Network (CNN) model that uses images captured from left and right cameras to predict the robot gripper's next movement; All the AI algorithms in that system are executed on a remote server, which the robot communicates with through Wi-Fi.

In this paper, we enhance the automated system's capabilities to manage complex path verification, boost power efficiency, and reduce latency in model prediction. Specifically, the system can now 1) detect and classify multiple fiber manipulation events with external random perturbations. 2) We design an LC-type duplex assembly with an improved accuracy tolerance. The modified LC duplex assembly enables the system to use a single central camera for fiber insertion without relying on CNN models. 3) Field programmable gate array (FPGA)-based control accelerates AI inference, enhancing the system's overall efficiency.

2. Innovation

Fig. 1a illustrates the experimental setup of an AI-powered robotic arm conducting automated operations. The robot has a 7-degree of freedom (DoF) collaborative robotic arm [2] that can work alongside or autonomously from human operators. A 2-finger gripper [3] is installed for handling a fiber adapter and connector and a built-in

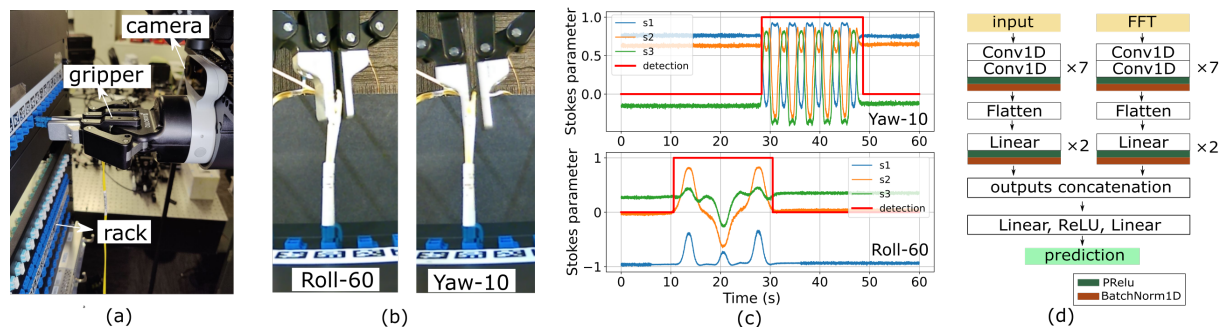


Fig. 1: (a) Image showing the robotic arm and fiber patch-panel rack; (b) Top view of the gripper rolling the fiber pigtail during the Roll-60 event and swinging the pigtail during the Yaw-10 event; (c) Stokes parameter traces for the Roll-60 and Yaw-10 events, with the detection model's output represented by the red line; (d) Model architecture used to classify between Roll-60, Yaw-10 and measurements involving no manipulation.

camera is positioned directly above the gripper. The robot performs fiber unplug and insertion on a 19" fiber patch-panel rack on which 1U fiber adapter panels with 24 LC duplex adapters are mounted. Duplex LC single-mode fiber cables for bi-directional communications are connected to the panels and interconnect S4X400H optical transponders (OTs) of a commercial Nokia 1830 PSS transport node (TN), configured via a software-defined networking (SDN) controller. Polarization tracking with an update rate of 5 ms runs at the OTs. Robot Operating System (ROS) [4] is implemented to facilitate sensor data publishing and robot control. The former receives commands from the latter to perform different tasks.

The three demos are described below:

2.1. Multiple events detection and classification

The detection of a single event using a real-time coherent receiver [5, 6] was successfully applied in basic path verification [1]. However, there are scenarios where multiple events need to be detected and analyzed for comprehensive path verification such as detecting shared risk group [7] under random environment perturbations. Fig. 1b illustrates two fiber manipulation events: Roll-60 and Yaw-10. In Roll-60, the 2-finger gripper loosely grips and rolls the fiber pigtail with a maximum angle of 60 degrees and repeats 1.5 cycles. In Yaw-10, the fiber pigtail is swung 5 cycles horizontally with a maximum angle of 10 degrees.

Detection We detect the events using the temporal traces of the Stokes parameters (s_1 , s_2 , and s_3 in Fig. 1c). We gathered a dataset of 180 Stokes measurements, each lasting 60 seconds. Two-thirds of these measurements include either the Roll-60 or Yaw-10 event, with each event occurring at a random offset within the measurement. The duration of both robot-driven events is around 22 seconds. The remaining one-third of the measurements do not involve any robotic fiber manipulation. The state of polarization was deliberately altered between the measurements. The dataset was divided into training, validation, and test sets, with proportions of 60%, 20%, and 20%, respectively. We utilize the same model as described in [1] for event detection. This model includes 1D convolutional layers, long short-term memory (LSTM) layers, upsampling layers, sigmoid layers, as well as ReLU and normalization layers. The model's output provides a binary weight for each temporal bin, with a higher weight indicating the event's location within the period. After training the model for 500 epochs, it achieved an accuracy of 97.5% on the validation data and 96.8% on the test data. Fig. 1c visualizes the Stokes parameter traces for the Roll-60 and Yaw-10 events, and the model's output is represented by the red line, which accurately detects and locates the events.

Classification We extracted 30-seconds from each of the 180 Stokes measurements as the input dataset. Two-thirds of these measurements include either the Roll-60 or Yaw-10 event and the remaining do not involve any robotic fiber manipulation. The dataset was divided into training, validation, and test sets, with proportions of 80%, 10%, and 10%, respectively. We applied a real-to-complex discrete Fourier transform to the input signals to generate FFT data. Both the original input data and the FFT data were then passed through seven blocks of two one-dimensional convolutional layers, a flatten layer, and two linear blocks, as depicted in Fig. 1d. Their outputs are concatenated and fed through a linear layer with ReLU activation, followed by an additional linear layer for making predictions. We trained the model using a one-cycle learning rate strategy, cross-entropy loss, and the Adam optimizer, with a batch size of 4. Impressively, the model achieved a 100% accuracy on both the validation and test datasets within 100 training epochs.

2.2. Efficient fiber insertion using modified LC duplex assembly

The images in Fig. 2a show that the unique ArUco markers [8] above duplex fiber adapters can be detected, and their position and orientation in relation to the gripper can be estimated by analyzing the pattern. When inserting a

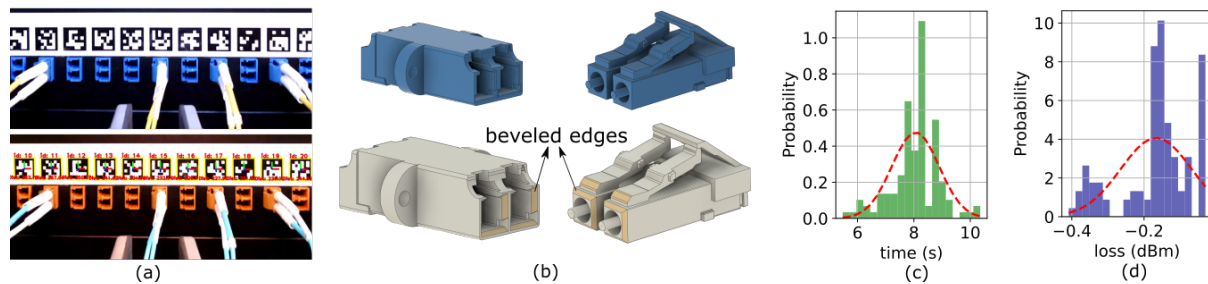


Fig. 2: (a) Image captured by the camera above the gripper (upper) and processed image showing marker detection (lower); (b) Comparison between the original LC duplex adapter and connector (blue) and their modified version (white); (c) Distribution of insertion duration; (d) Distribution of power loss.

connector longitudinally into an adapter from a distance of 60 mm, the accuracy of pose estimation for its marker in both vertical and horizontal directions is within 0.75 mm. The robotic arm, with a repeatability of 0.1 mm, necessitates an insertion tolerance of at least 0.85 mm to ensure successful insertion. We made modifications to the shape of both the LC connector and the adapter and increased their beveled edges by 0.45 mm offset, as illustrated in Fig. 2b. The difference between the adapter's openness and the width of the connector is less than 0.2 mm. As a result, the insertion tolerance, which is approximately 1.0 mm, exceeds the required 0.85 mm and should be appropriate for the insertion.

To evaluate the insertion efficiency, we initiated it from a longitudinal distance of 60 mm and a randomly generated starting position with a maximum horizontal and vertical distance of 3 mm to the adapter. In the alignment stage, the gripper first adjusts its longitudinal orientation to match the adapter series, fine-tunes its horizontal and vertical positions to maintain precise alignment with the adapter, and then moves to a distance of 8 mm from the adapter. During the insertion stage, we set the step length to 1.5 mm with a 0.2 seconds interval between steps while continuously monitoring the actuators' torque of the robotic arm. The insertion is considered complete when the gripper encounters significant resistance, as indicated by a torque reading on the actuator 4 exceeding 19.5 Nm. The process achieves a 100% success rate over in total of 120 trials, with an average alignment duration of 22.9 seconds. Fig. 2c displays an average insertion duration of 8.1 seconds, which is 10 seconds shorter than when using a CNN model [1]. Fig. 2d illustrates that the average loss is 0.17 dBm, indicating that the modification has a negligible impact on the mating mechanism.

2.3. AI inference acceleration using an FPGA

The remote server control discussed in the previous work [1] is well-suited for handling complex tasks that require significant computational power and straightforward software modification. To expand our system's capabilities, we introduce FPGA-based control using the *Vitis*TM AI platform [9] from AMD to improve power efficiency and reduce low latency. The camera-guided fiber insertion model described in [1] is inspected, quantized, and compiled before being deployed on *Zynq*TM UltraScale+ KV260 [10]. Negligible accuracy degradation is observed after quantization from the floating-point graphics processing unit (GPU) model [1] to an FPGA deployable fixed-point 8-bit model.

3. OFC Relevance And Demo Content

Leveraging the spatial domain and spatial switching to scale optical network capacity [11], employing optical networks for environmental sensing [12] and AI assistance in optical network operation and maintenance [13] are all being actively investigated. This paper covers a robotic passive fiber cross-connect, fiber path verification employing real-time coherent receivers and AI inference acceleration, which are well aligned with the research interests in photonics society and OFC.

Three demos will be presented to the OFC audience. We will begin with the introduction of ROS programming and robot control mechanism applied in the demos, and illustrate the architecture and operation of the system. Attendees will have the opportunity to remotely control a robot to perform various tasks. The first two demos will be delivered through real-time video streaming, with two video streams displayed on the monitors. One stream shows the robot's actions in front of the fiber patch panel, as depicted in Fig. 1a. The other displays the video captured by the built-in central camera on the robotic arm, along with a virtual overlay after marker detection, as depicted in Fig. 2a. The AI inference acceleration demo will be demonstrated on-site using an FPGA.

References

1. X. Xu *et al.*, "Automated Fiber Switch with Path Verification Enabled by An AI-Powered Multi-Task Mobile Robot", Proc. ECOC, 2023, paper Th.C.2.7.
2. KINOVA, <https://www.kinovarobotics.com/product/gen3-robots/>
3. ROBOTIQ, <https://robotiq.com/products/2f85-140-adaptive-robot-gripper/>
4. ROS, <https://www.ros.org/>
5. F. Boitier *et al.*, "Proactive Fiber Damage Detection in Real-Time Coherent Receiver.", Proc. OFC 2017, pp. 1-3.
6. M. Mazur *et al.*, "Field Trial of FPGA-Based Real-Time Sensing Transceiver over 524 km of Live Aerial Fiber", Proc. OFC 2023, paper Tu3G.4.
7. Y. Li *et al.*, "Research and Experiment on AI-based Co-cable and Co-trench Optical Fibre Detection", Proc. ECOC 2023, pp. 1-4.
8. Detection of ArUco Markers, https://docs.opencv.org/4.x/d5/dae/tutorial_aruco_detection.html
9. Vitis AI, <https://www.xilinx.com/products/design-tools/vitis/vitis-ai.html>
10. Kria KV260, <https://www.xilinx.com/products/som/kria/kv260-vision-starter-kit.html>
11. D. M. Marom *et al.*, "Optical Switching in Future Fiber-Optic Networks Utilizing Spectral and Spatial Degrees of Freedom", Proc. of the IEEE, 110(11), 1835-1852, 2022.
12. M. Cantono *et al.*, "Optical Network Sensing: Opportunities and Challenges", Proc. OFC 2022, paper M2F.1.
13. X. Xu *et al.*, "Optical network diagnostics using graph neural networks and natural language processing", Proc. OFC 2023, paper M3G.5.